



Extended validation of Aeolus winds with wind-profiling radars in Antarctica and Arctic Sweden

Sheila Kirkwood¹, Evgenia Belova¹, Peter Voelger^{1*}, Sourav Chatterjee², Karathazhiyath Satheesan³

1 Swedish Institute of Space Physics, Kiruna, SE-98128, Sweden

5 2 National Centre for Polar and Ocean Research, Ministry of Earth Sciences, Vasco da Gama, Goa, 403804, India

3 Department of Atmospheric Sciences, School of Marine Sciences Cochin University of Science and Technology, Cochin, Kerala, 682 016, India

*Correspondence to: Peter Voelger (peter.voelger@irf.se)

Abstract. Winds from two wind profiling radars, ESRAD in Arctic Sweden and MARA on the coast of Antarctica, are compared with collocated winds measured by the Doppler lidar onboard the Aeolus satellite for the time period July 2019 - May 2021. Data is considered as a whole, and subdivided into summer/winter and ascending (afternoon) /descending (morning) passes. Mean differences (bias) and random differences are categorised (standard deviation and scaled median absolute deviation) and the effects of different quality criteria applied to the data are assessed, including the introduction of the ‘modified Z-score’ to eliminate gross errors. This last criterion has a substantial effect on the standard deviation, particularly for Mie winds. Significant bias is found in two cases, for Rayleigh/descending winds at MARA (-1.4 (± 0.7) m/s) and for all Mie winds at ESRAD (+1.0 (± 0.3) m/s). For the Rayleigh wind bias at MARA, there is no obvious explanation for the bias in the data distribution. For the Mie wind at ESRAD there is a clear problem with a distribution of wind differences which is skewed to positive values (Aeolus HLOS wind > ESRAD wind). Random differences (scaled median absolute deviation) for all data together are 5.9 / 5.3 m/s for Rayleigh winds at MARA/ESRAD respectively, and 4.9 / 3.9 m/s for Mie winds. These represent an upper bound for Aeolus wind random errors since they are due to a combination of spatial differences, and random errors in both radar winds and Aeolus winds.

1 Introduction

The Aeolus satellite mission is the first attempt to measure meteorological wind profiles on a global scale from space using the doppler lidar technique. It carries a single instrument - the Atmospheric Laser Doppler Instrument (ALADIN) - which uses two detectors to measure backscattered laser light from cloud/aerosol particles (Mie scatter) and molecules (Rayleigh scatter), respectively (Stoffelen et al., 2005; ESA, 2008; Reitbuch, 2012). It was launched on 22 August 2018 and, from the planning stage, a wide range of validation tests were proposed, comparing the wind profiles from the satellite with those measured by established techniques such as radiosondes, ground-based radars and lidars.



30 The validation tests have led to a number of revisions of the processing algorithms after the launch, to account for unexpected instrumental effects. For example, validation exercises soon after the start of the mission identified temperature-dependent effects on the mirror in the instrument, with subsequent changes to the data-processing giving substantial improvement of the biases from more than 5 m/s (Martin et al., 2021; Rennie and Isaksen, 2020) to less than 2 m/s. This allowed the Aeolus winds to make a positive contribution to global weather forecasting (Reitebuch et al., 2020; Rennie et al., 2021; Weiler et al., 2021). A good number of validation comparisons using the corrected data-processing after 2020
35 (baselines 2B10 and later) have been reported, as summarised in e.g. Wu et al. (2022), Ratynski et al. (2022), which mostly indicate possible biases less than 1 m/s and random errors 4-7 m/s for Rayleigh winds, 2-4 m/s for Mie winds. At the same time, the biases and random errors seem to vary more than might be expected between the different measurement techniques and locations used in the validations. Lux et al. (2022) have looked in detail at the non-random nature of differences between Aeolus winds and reference winds and suggest that the exact details of quality control applied in validation studies can
40 significantly affect the results. The bias and random error estimates can be affected by small numbers of outliers, particularly for Mie winds where large errors outside a Gaussian distribution (gross errors) can be caused by misinterpretation of noise as signal. This can lead to predominantly positively-biased gross errors.

An initial validation comparing measurements from two wind-profiler radars in Arctic Sweden and in Antarctica, with Aeolus winds processed with the 2B10 baseline, was published by Belova et al. (2021). This found biases < 2 m/s, and
45 standard deviation of the differences between satellite and radar winds in the range 4-7 m/s. Note that a large bias first reported for Mie winds in the data for Antarctica was found to be in error as detailed in the Corrigendum published in May 2022 (Belova et al., 2021, Corrigendum). However, the available time period for comparison was short (only 6 months) and uncertainties in the biases were large. Almost 2 years of data from these high-latitude radars are now available for comparison with the longest available consistently processed Aeolus data set (baseline 2B11), from July 2019 to May 2021.
50 A comparison of these extended data sets, together with more detailed consideration of the statistics as suggested by Lux et al. (2022) is presented here.

2 Overview of measurements and quality criteria

The radars used are MARA, situated at Maitri in Antarctica (70.77° S, 11.73° E) and ESRAD, situated near Kiruna in Arctic Sweden (67.88° N, 21.10° E). Full details of the radar and satellite operation modes and the available data can be found in
55 Belova et al. (2021). In summary, we select all satellite measurement tracks passing within 100 km from each radar site. For Aeolus Rayleigh (clear) winds, we then select the profile with the mean position closest to the radar (which is averaged over about 87 km along the track). For Aeolus Mie (cloudy) winds, which are averaged over about 14 km of track, we collect all observations within 100 km of the radar and average them within the same height bins as the corresponding Rayleigh profile. We use the horizontal line-of-sight ('hlos') winds from the Level_2B data-product, here using the 2B11 baseline. Radar
60 measurements of the full wind vector are averaged from 30 minutes before the pass, to 30 minutes after the pass, again to the same height bins as the Rayleigh wind profile. Radar 'hlos' winds are calculated from the radar vector winds (ignoring the



vertical component, which is found to be negligible in the 1 h averages). There are usually 4 Aeolus passes per week providing comparative data at MARA, 3 passes per week at ESRAD.

65 For the analysis in Belova et al. (2021) only winds less than 100 m/s (radar and Aeolus), validity flag =1 (Aeolus) and with estimated random error (EE) < 8 m/s (Rayleigh), EE < 5 m/s (Mie), and 95% confidence limit < 2 m/s (radar) were used. Here, as suggested by Lux et al. (2022), we first examine the statistics of the differences between radar and Aeolus winds for different quality criteria (QC). Differences are parameterised in terms of bias, standard deviation (SD), scaled median absolute deviation (ScMAD), where

$$bias = \frac{1}{N} \cdot \sum_{i=1}^N (HLOS_{Aeolus,i} - HLOS_{radar,i}) \quad (1)$$

70
$$SD = \sqrt{\frac{1}{N-1} \sum ((HLOS_{Aeolus,i} - HLOS_{radar,i}) - bias)^2} \quad (2)$$

$$ScMAD = 1.4826 \cdot median(|(HLOS_{Aeolus,i} - HLOS_{radar,i}) - median(HLOS_{Aeolus,i} - HLOS_{radar,i})|) \quad (3)$$

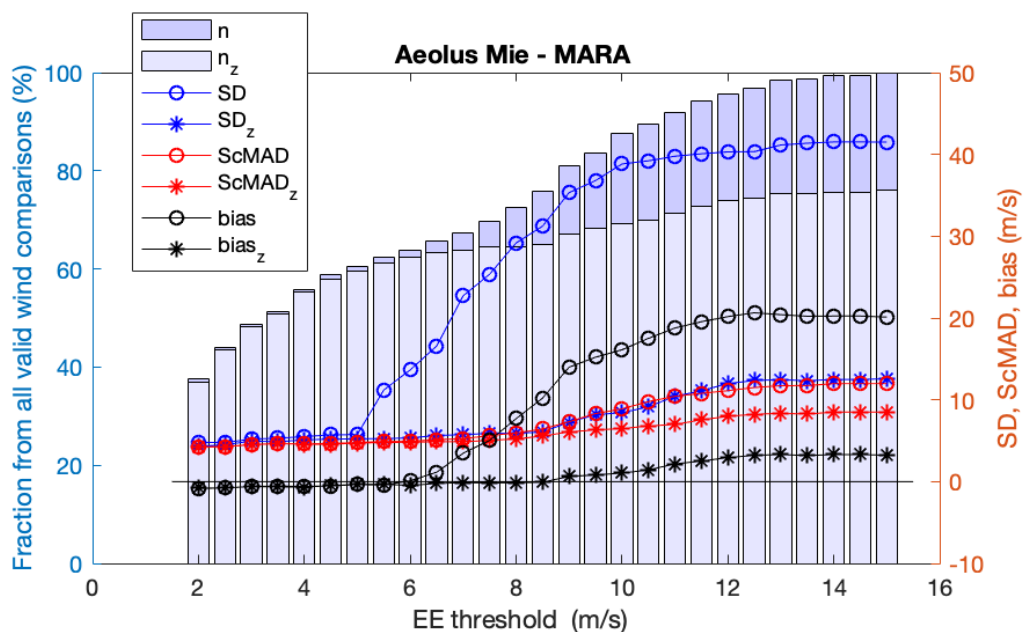
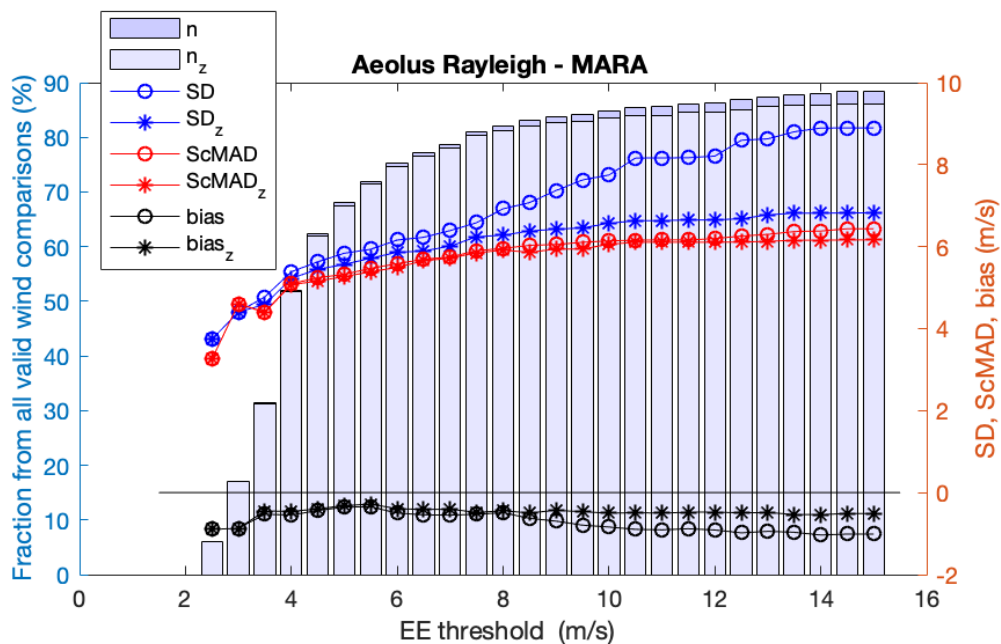
Both SD and ScMAD are estimates of the variability of the wind error but ScMAD is less susceptible to outliers. If the distribution is gaussian, they have the same value.

In order to determine suitable QC, we first look at these parameters as a function of EE threshold for Rayleigh and Mie
75 winds, and with and without a second QC, designed to eliminate gross errors, based on the modified Z-score (ModZ) (Iglewicz and Haglin, 1993), as suggested by Lux et al (2022).

$$ModZ_i = \frac{|(HLOS_{Aeolus,i} - HLOS_{radar,i}) - median(HLOS_{Aeolus,i} - HLOS_{radar,i})|}{ScMAD} \quad (4)$$

Figure 1 shows the fraction of possible comparison points (n) retained, biases, SD and ScMAD as a function of the EE threshold used for rejection, at MARA. Parameters with subscript z (n_z , $bias_z$, SD_z , $ScMAD_z$) have been calculated after
80 further rejecting data points with $ModZ_i > 3.5$. Values for this limit between 3.0 and 3.5 were found to lead to a high degree of normality for differences between Aeolus observations and ECMWF background winds by Lux et al. (2022). We have also tested rejecting $ModZ_i > 3.0$, but the differences are very small so we show only results using $ModZ_i > 3.5$.

In Figure 1, for Rayleigh winds it is clear that SD rises steeply for $EE > 7$ m/s but this is much less apparent where the check on $ModZ_i$ has removed outliers (SD_z). ScMAD is insensitive to the $ModZ_i$ restriction and is close to SD_z up to 8 m/s
85 suggesting a close to Gaussian distribution after the $ModZ_i$ restriction. Bias and $bias_z$ are consistently small (about -0.5 m/s) from $EE > 3.5$ m/s up to 8 m/s and $bias_z$ remains at this level for all EE thresholds tested. Thus, the original choice of $EE < 8$ m/s as the QC for Rayleigh winds seems reasonable. For Mie winds at MARA, both SD and bias increase sharply for $EE > 5$ m/s. $ScMAD_z$ and SD_z remain very close to each other up to $EE < 8.5$ m/s. $bias_z$ remains small and at rather constant





90 **Figure 1: Comparison of Aeolus HLOS winds with MARA, upper panel for Rayleigh-clear winds, lower panel for Mie-cloudy. Plots show the fraction of possible comparison points (n) retained, biases, SD and ScMAD as a function of the EE threshold used for rejection. Subscript z (n_z , $bias_z$, SD_z , $ScMAD_z$) show results after further rejecting data points with $ModZ > 3.5$.**

level from $EE < 5$ to $EE < 8.5$ m/s. So, in order to include as many points as possible and a distribution as close as possible to gaussian, it seems reasonable to increase the original threshold of $EE < 5$ m/s for Mie winds, to anywhere up to $EE < 8$ m/s together with the outlier rejection using $ModZ_i < 3.5$.

95 Figure 2 shows corresponding plots at ESRAD. For Rayleigh winds, the bias and $bias_z$ are insensitive to the EE threshold from $EE < 5$ m/s to $EE < 15$ m/s. SD increases sharply at $EE < 10$ m/s and above. Otherwise, SD_z , $ScMAD$, $ScMAD_z$ and the difference between SD_z and $ScMAD_z$ all increase slowly but steadily for all EE thresholds above $EE < 5$ m/s. Thus, there is no clear motivation for a particular choice of EE threshold for Rayleigh winds. For Mie winds at ESRAD, SD and bias increase rapidly with EE thresholds > 5 m/s while SD_z , $ScMAD$, $ScMAD_z$ and the difference between SD_z and $ScMAD_z$ seem to
100 increase more rapidly for EE threshold > 7.0 m/s. The $bias_z$ increases slowly across all EE thresholds but is fairly constant between $EE < 5$ m/s and $EE < 7$ m/s.

Figures 1 and 2 show very similar behaviour at MARA and at ESRAD so there is no obvious reason to treat the data from the two sites differently. Thus, in the following we adopt QC using only Aeolus winds with estimated random error (EE) < 8 m/s (Rayleigh), < 7 m/s (Mie) and rejecting likely gross errors where $ModZ > 3.5$. The same restrictions on radar winds as
105 previously are also applied - wind speed less than 100 m/s and 95% confidence limit < 2 m/s

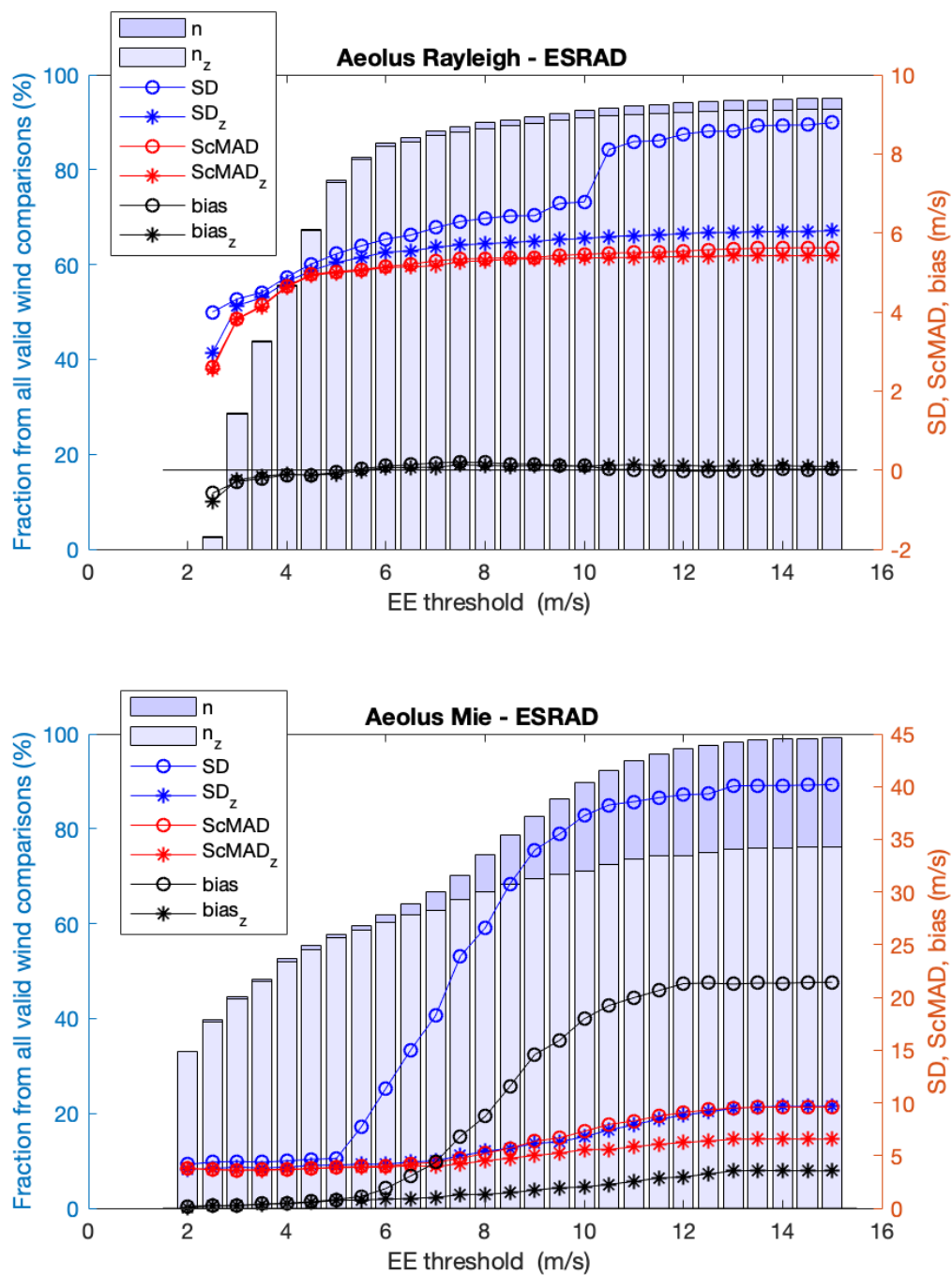


Figure 2: As Figure 1 but for ESRAD.



Table 1: Statistics of correlation differences between Aeolus Rayleigh-clear HLOS winds and MARA HLOS winds. N_z is the number of comparison points passing all quality checks (QC, see text for details), % outliers is the number of points rejected by the final QC ($\text{Mod}Z < 3.5$, Eq. 4). slope_z is the slope of the best-fit straight line correlation, bias_z , SD_z and ScMAD_z are as defined in Eqs. 1-3. Columns are for all data (July 2019 - May 2021), or divided into summer (24 September-22 March), winter (23 March-23 September), descending and ascending passes. Values between square brackets [] are 95% confidence limits.

Rayleigh-MARA	all	summer	winter	descending	ascending
N_z	737	553	294	351	387
% outliers	1.1	1.1	1.0	0.8	1.0
correlation_z	0.77	0.78	0.77	0.68	0.77
slope_z	0.90 [0.84 0.95]	0.92 [0.85 0.99]	0.89 [0.80 0.97]	0.93 [0.82 1.03]	0.98 [0.89 1.05]
bias_z	-0.5 [-0.9 0.0]	0.0 [-0.6 0.6]	-0.8 [-1.6 -0.1]	-1.4 [-2.1 -0.7]	0.6 [0.0 1.1]
SD_z	6.3	6.2	6.3	6.8	5.8
ScMAD_z	5.9	5.8	5.9	6.8	5.5

Table 2: As Table 1, but for Aeolus Mie-cloudy HLOS winds and MARA HLOS winds.

Mie-MARA	all	summer	winter	descending	ascending
N_z	312	208	102	146	165
% outliers	5.2	4.1	8.9	2.7	7.8
correlations_z	0.86	0.87	0.84	0.78	0.70
slope_z	0.96 [0.89 1.01]	0.90 [0.83 0.96]	1.11 [0.97 1.25]	0.94 [0.81 1.06]	0.99 [0.84 1.13]
bias_z	-0.1 [-0.8 0.5]	0.1 [-0.6 0.8]	-0.6 [-1.9 0.7]	-0.4 [-1.3 0.4]	-0.2 [-1.1 0.8]
SD_z	5.7	5.0	6.6	5.1	6.2
ScMAD_z	4.9	4.6	6.4	4.2	5.3

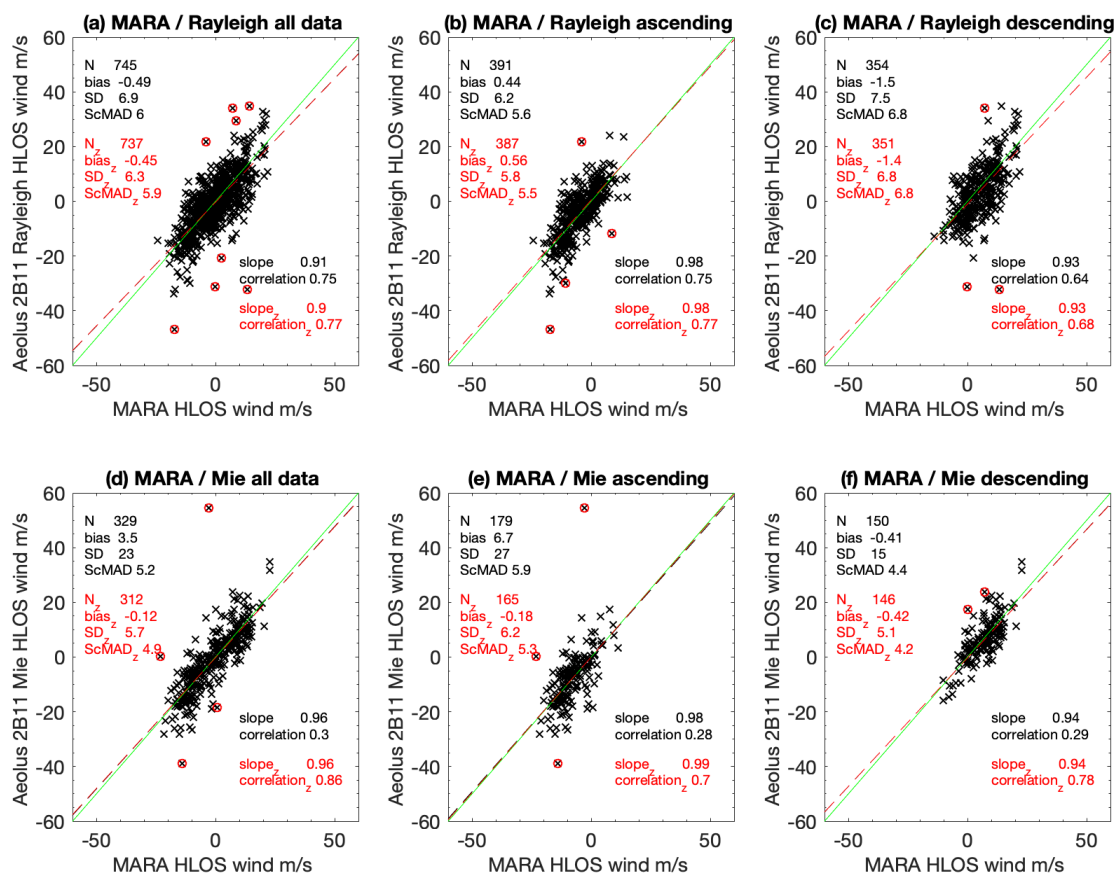


Figure 3: Scatter plots of Aeolus HLOS Rayleigh-clear winds (a-c) and Mie-cloudy winds (d-f) vs MARA winds. (a),(d) show all orbits together, (b),(e) in and data show ascending passes and (c),(f) descending passes. Red circles show data points removed by the $ModZ > 3.5$ QC criterion. Parameters in black/red indicate fits including/excluding these points. Green line is where Aeolus wind is exactly equal to MARA wind.



3 Comparison with MARA radar, Antarctica

Statistics of the comparison between Aeolus and MARA are given in Table 1 (Rayleigh winds) and Table 2 (Mie winds), and scatter plots of the comparisons are shown in Figure 3. The first column in each table shows the comparison for all of the data, corresponding to Fig. 1 at EE thresholds 8 m/s for Rayleigh winds, 7 m/s for Mie winds. The tables also show the results after dividing the data by season (summer, 23 September - 22 March and winter 23 March - 22 September) and by ascending (afternoon) / descending (morning) Aeolus passes. Variations of, for example, solar illumination on the ground between summer and winter and opposite lidar backscatter direction relative to the prevailing wind between ascending and descending passes could in principle affect the comparison.

For the Rayleigh winds, Table 1 shows that there are no significant differences between summer and winter. There does seem to be a significant difference between ascending and descending passes with descending passes showing lower correlation, stronger (negative) bias and higher SD_z and $ScMAD_z$. These differences can also be discerned comparing Figs 3b and 3c. For all of the data together, there is a small, marginally significant bias. As can be seen in Fig.1, this bias is largely independent of the choice of EE threshold for data rejection.

For the Mie winds, Table 1 shows that there are (in %) twice as many outliers rejected by the $ModZ < 3.5$ QC in winter compared to summer, SD_z and $ScMAD_z$ are also higher in winter, but the biases are not significantly different. Ascending passes show a higher rate of outliers, and higher $SD_z/ScMAD_z$ compared to descending, but again with no significant bias for either. Again the differences can be discerned comparing Figs 3e and 3f. The differences in variability between ascending and descending passes are opposite for Mie winds compared to Rayleigh winds, the differences in variability between summer and winter affect only the Mie winds and significant bias for the descending passes affects only the Rayleigh winds, so they are unlikely to be explained by meteorology or by systematic errors in radar wind speed. Overall, SD_z and $ScMAD_z$ are slightly higher for Rayleigh winds (around 6 m/s) than for Mie winds (around 5 m/s). Comparing the red and black numbers in Figure 3 also shows the large change in SD and bias for Mie winds when the $ModZ < 3.5$ QC is applied (comparing $bias/SD$ with $bias_z/SD_z$).

Figure 4 shows height-resolved $bias_z$ and $ScMAD_z$ for the Aeolus-MARA comparison. The negative bias for Rayleigh descending winds is seen at almost all heights, although the uncertainties in the bias become very large above 6 km height. It is partly balanced by a positive bias (marginally significant) for the ascending passes so that, for all data together, the mean bias becomes closer to zero. For the Mie winds, with notably more restricted height coverage, there is no significant bias at any height.

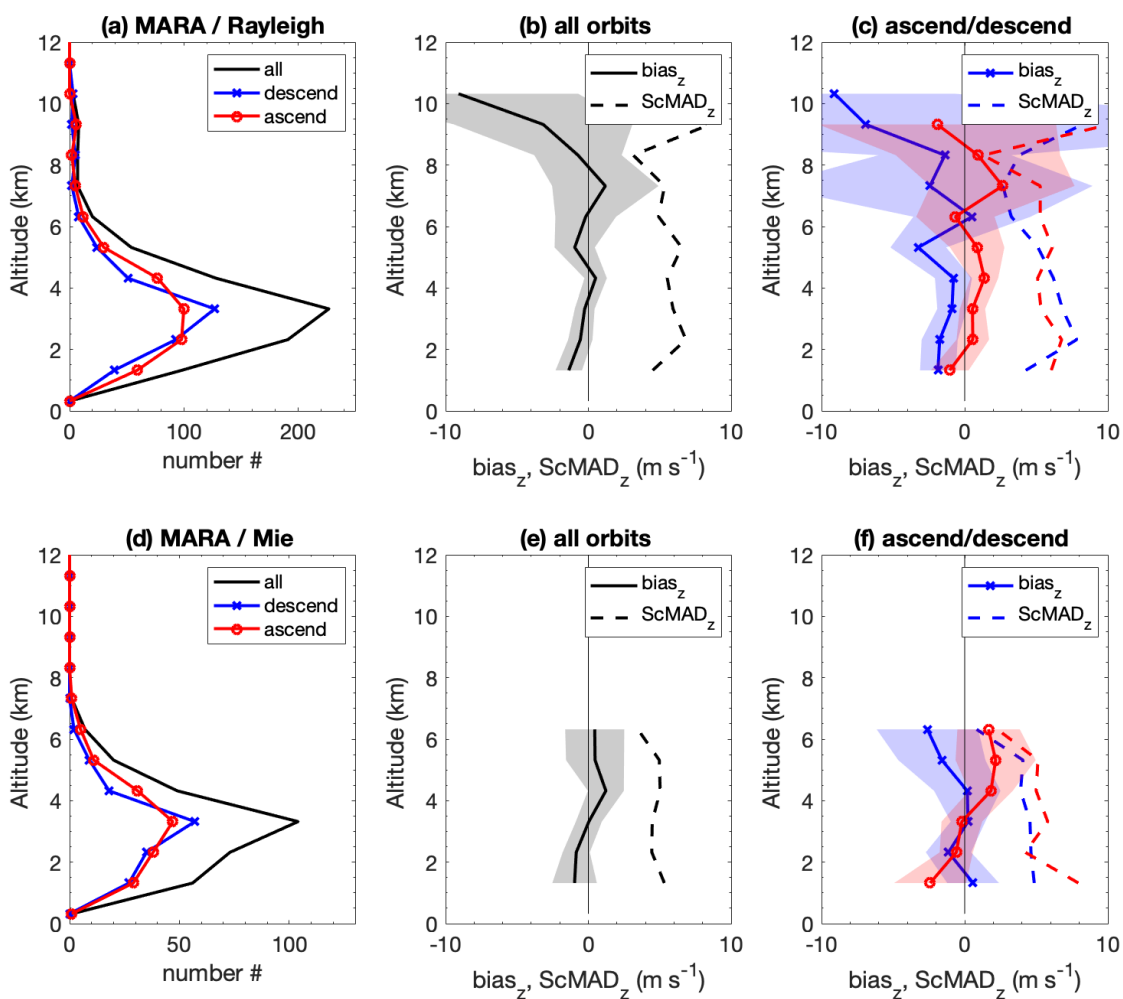


Figure 4: Comparison of Aeolus winds with MARA. Height profiles of (a),(d) number of data points, (b),(e) bias_z and ScMAD_z for all orbits together, and (c),(f) bias_z and ScMAD_z separately for ascending and descending passes.



Table 3: Statistics of correlation differences between Aeolus Rayleigh-clear HLOS winds and ESRAD HLOS winds. N_z is the number of comparison points passing all quality checks (QC, see text for details), % outliers is the number of points rejected by the final QC ($\text{ModZ} < 3.5$, Eq. 4). slope_z is the slope of the best-fit straight line correlation, bias, SD_z and ScMAD_z are as defined in Eqs. 1-3. Columns are for all data (July 2019 - May 2021), or divided into summer (23 March-23 September), winter (24 September-22 March), descending and ascending passes. Values between square brackets [] are 95% confidence limits.

Rayleigh-ESRAD	all	summer	winter	descending	ascending
N_z	1854	959	895	1220	634
% outliers	1.4	1.0	1.9	1.2	1.9
correlation_z	0.87	0.84	0.88	0.82	0.83
slope_z	0.99 [0.96 1.01]	1.00 [0.96 1.04]	0.96 [0.93 1.00]	0.97 [0.93 1.00]	0.96 [0.91 1.01]
bias_z	0.1 [-0.1 0.4]	0.3 [-0.1 0.7]	-0.1 [-0.4 0.3]	-0.0 [-0.4 0.3]	0.4 [0.0 0.9]
SD_z	5.7	5.9	5.5	5.8	5.6
ScMAD_z	5.3	5.4	5.1	5.2	5.2

Table 4: As Table 3, but for Aeolus Mie-cloudy HLOS winds and ESRAD HLOS winds.

Mie-ESRAD	all	summer	winter	descending	ascending
N_z	661	362	300	402	259
% outliers	5.7	3.7	3.0	4.0	2.6
correlation_z	0.91	0.89	0.92	0.86	0.89
slope_z	0.94 [0.91 0.97]	0.85 [0.80 0.89]	1.03 [0.98 1.07]	0.92 [0.86 0.97]	0.93 [0.87 0.98]
bias_z	1.0 [0.7 1.4]	1.1 [0.6 1.5]	1.0 [0.5 1.6]	1.1 [0.6 1.6]	0.9 [0.4 1.4]
SD_z	4.5	4.3	4.8	4.8	4.0
ScMAD_z	3.9	3.9	4.1	4.0	4.0

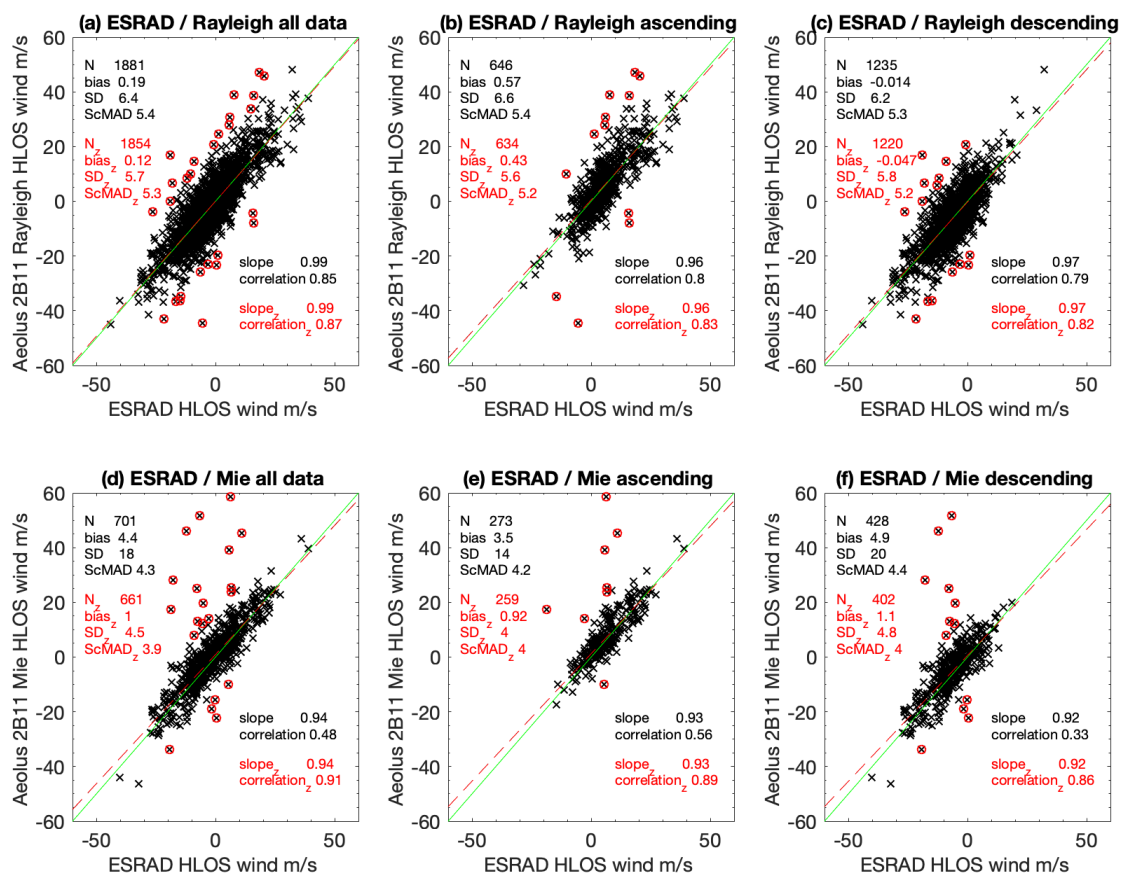


Figure 5: As Figure 3 but for ESRAD

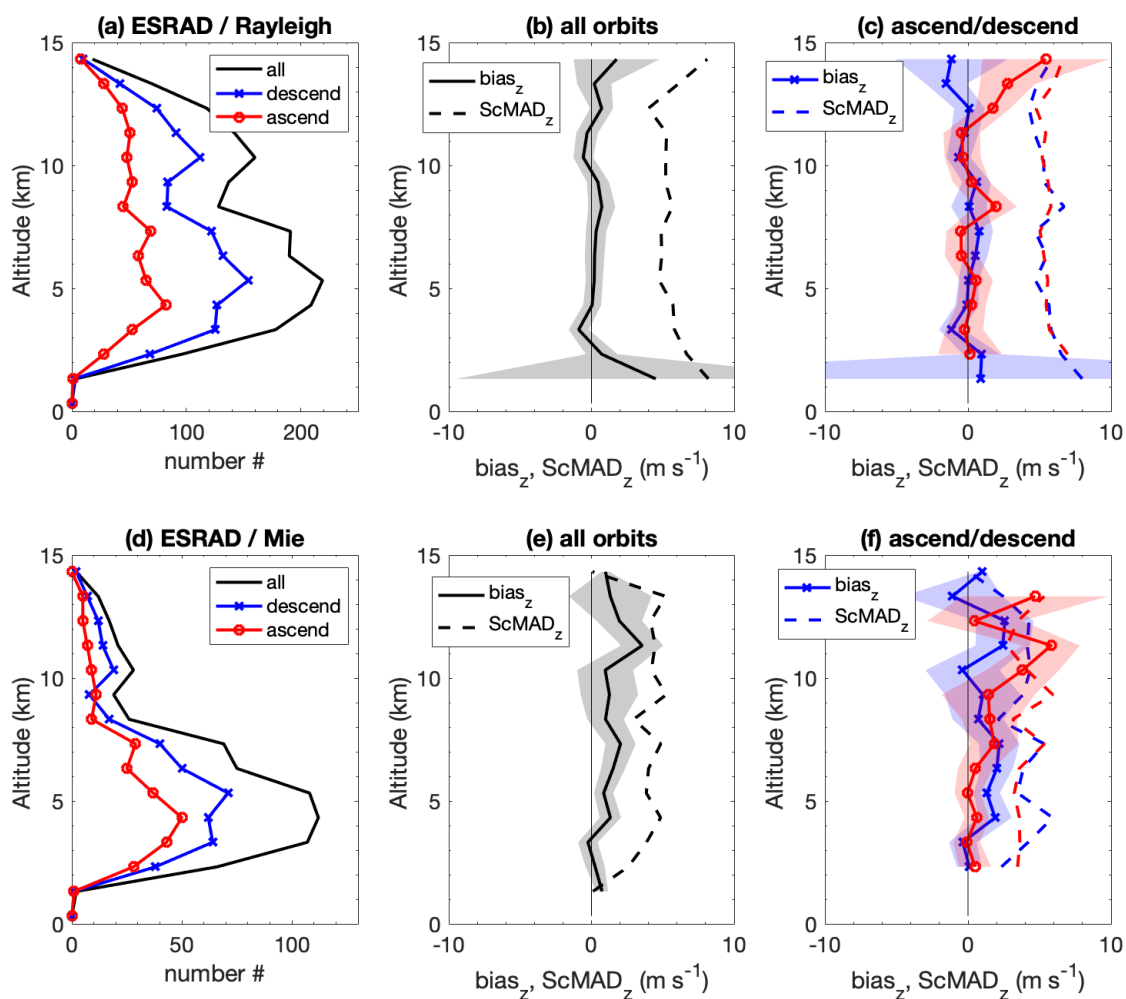


Figure 6: As Figure 4 but for ESRAD



4 Comparison with ESRAD radar, Arctic Sweden

- 135 Table 3 (Rayleigh winds) and Table 4 (Mie winds) show statistics of the comparison between Aeolus and ESRAD. Scatter plots of the comparisons are shown in Figure 5. The comparison for all of the data is shown in the first column in each table, corresponding to Fig. 2 at EE thresholds 8 m/s for Rayleigh winds, 7 m/s for Mie winds. The tables also show the results after dividing the data by season (winter, 23 September - 22 March and summer 23 March - 22 September) and by ascending (afternoon) / descending (morning) Aeolus passes.
- 140 In Table 3 (Rayleigh winds), there are no significant differences between summer and winter, or between ascending and descending passes, and $bias_z$ in all cases is not significantly different from zero. In Table 4 (Mie winds), there are again no significant differences between summer and winter or between ascending and descending passes. However, there is a significant bias of about 1 m/s for all cases. Overall, SD_z and $ScMAD_z$ are slightly higher for Rayleigh winds (around 5 m/s) than for Mie winds (around 4 m/s), and slightly lower than at MARA.
- 145 Figure 5 illustrates the distribution of points about the regression lines and shows how the rejection of points with $ModZ > 3.5$ has effectively eliminated several gross errors. Figure 5 (comparing the black numbers for $bias/SD$ with the red numbers for $bias_z/SD_z$) also shows the large change in SD and bias for Mie winds when the $ModZ < 3.5$ QC is applied. Figure 6 provides height-resolved profiles of $bias_z$ and $ScMAD_z$. Above 6 km height, the bias uncertainties are notably lower than at MARA - this is a result of a much larger number of comparison points thanks to the higher power of the ESRAD radar. For Rayleigh winds there is no significant bias at any height, for Mie winds the ~ 1 m/s positive bias identified in Table
- 150 4 is clearly seen at all heights. From Fig. 2 it is clear that a positive bias appears whatever the EE threshold.

5 Further analysis of non-zero biases

- The analysis above has identified significant non-zero biases in two cases - for Rayleigh winds at MARA (descending passes, $bias_z$ -1.4 m/s) and for all Mie winds at ESRAD ($bias_z$ +1 m/s). To check these further, we plot normal probability
- 155 curves for a series of EE thresholds in Figures 7 and 8. These plots compare the distribution of the data (Aeolus hlos wind - radar hlos wind, after applying the $ModZ < 3.5$ QC) to the normal distribution ('+'). A reference line (red) joins the first and third quartiles of the data and is projected to the ends of the data. If the sample data has a normal distribution, then the data points appear along the reference line. Departures from the line to the right at the positive end and to the left at the negative end show 'fat tails' (more points in the tails of the data distribution than in the normal distribution). When one tail is bigger
- 160 than the other the distribution is skewed. Figure 7 (Rayleigh-descend - MARA) shows fairly symmetric, small fat tails which grow slightly as the EE threshold is increased. The bias remains the same over the range of EE thresholds. This same constant bias over all EE thresholds can be seen for all of the Rayleigh-MARA winds in Figure 1. Figure 8 (Mie - ESRAD) shows small fairly symmetric fat tails for low values of the EE threshold but these grow large and become skewed at the higher EE thresholds, leading to an increase
- 165 in the bias estimate. This is also seen in Figure 2.

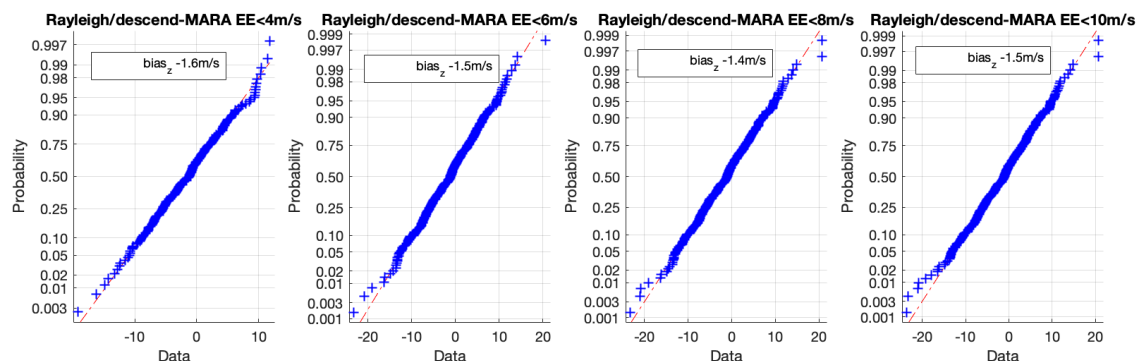


Figure 7: Normal probability plot for ('Data') the difference between Aeolus Rayleigh HLOS wind and MARA wind (descending passes) for a series of EE thresholds, after rejecting points with ModZ > 3.5. See text for details.

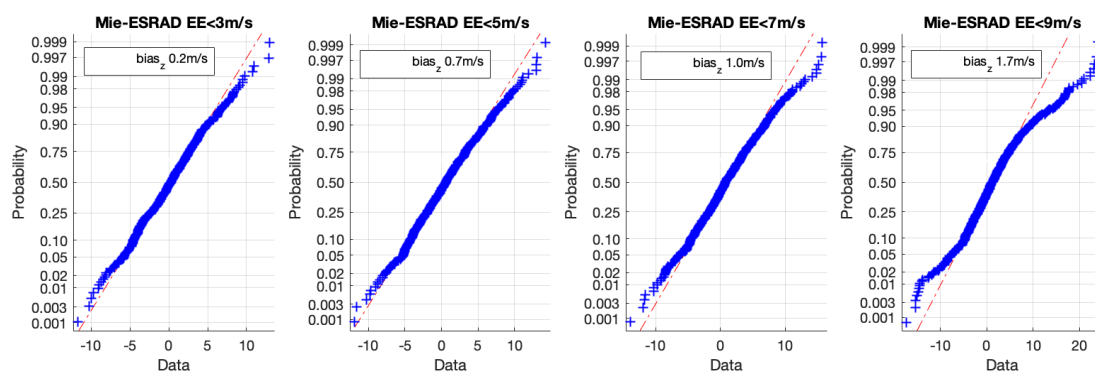


Figure 8: Normal probability plot for ('Data') the difference between Aeolus Mie HLOS wind and ESRAD wind (all passes) for a series of EE thresholds, after rejecting points with ModZ > 3.5. See text for details.

6 Discussion and Conclusions

In the present study we have compared 2 years of wind measurements by the Aeolus satellite (Rayleigh-clear and Mie-cloudy) with winds from two wind-profiler radars in Arctic Sweden and in coastal Antarctica, respectively. For each radar we have looked at ascending and descending passes and summer and winter separately, as well as for all of the data together.

170 We have identified significant non-zero biases in only two subsets of the data - for Rayleigh winds at MARA (winter descending passes, bias -1.4 m/s) and for Mie winds (all passes) at ESRAD (bias +1 m/s). Biases for all other subsets are not different from zero at the 95% confidence limits. In the initial validation of Aeolus winds against the MARA radars (Belova et al, 2021) significant bias (-2 m/s) was also found for Rayleigh winds (descending passes) at MARA which is similar to the result here. For Mie winds (Belova et al, 2021, corrigendum), the initial study also found a positive bias similar to the



175 present study at ESRAD (average +1.2 m/s). The number of comparison points has increased by about a factor 3 in the
present study due the longer time period (two years instead of 6 months) and, for Mie winds, the relaxation of the random
error (EE) threshold for rejection of data from 5 m/s to 7 m/s. With the increase in numbers and the introduction of a new
180 criterium for rejection of outliers ($\text{mod}Z < 3.5$), the uncertainties in the bias estimates have been substantially reduced (from
1-3 m/s to 0.3 – 1 m/s) so we can be more confident that the estimated biases are accurate. It seems clear that uncorrected
biases can still appear for our particular locations even after the data processing improvements incorporated in the L2B
product with 2B11 baseline. In addition, for Mie winds at ESRAD there is clearly a problem with a skewed distribution of
random errors, with substantial numbers of Mie (HLOS) winds which are greater in magnitude than the radar winds, larger
than expected for a normal distribution, and which are difficult to remove even with the new outlier constraint ($\text{mod}Z < 3.5$).
The biases are similar in magnitude to results from other locations (e.g. Wu et al., (2022) Ratynski et al. (2022) and
185 summaries included in those papers). The problem of skewness for Mie winds has also been reported, and addressed in
detail, by Lux et al. (2022).

Random differences (ScMAD_z) for all data together are 5.9 / 5.3 m/s for Rayleigh winds at MARA/ESRAD respectively, and
4.9 / 3.9 m/s for Mie winds. Slightly lower values at ESRAD than at MARA can be attributed to the higher power of the
ESRAD radar which gives higher accuracy for the ESRAD radar winds. The difference between Rayleigh and Mie winds is
190 expected because of different random errors in those wind estimates from Aeolus.

For the MARA and ESRAD data, Belova et al. (2021) reported SD values for different subsets in the range 4-6 m/s for
Rayleigh winds, and mostly 3-5 m/s for Mie winds. The present study shows SD_z 5.5 - 6.8 for Rayleigh winds, 4.0 - 6.6 m/s
for Mie winds, which are somewhat higher. The increase in SD is in line with the increase in estimated random errors for
Aeolus winds between June 2019 and June 2021 (2B11 baseline) shown by Lux et al. (2022) , which is due to degradation
195 in power of the Aeolus lidar. The absolute values of SD_z here are 1-2 m/s higher than expected for Aeolus random errors,
 ScMAD_z values a little closer. SD_z and ScMAD_z are a combination of spatial effects (radars and Aeolus are not measuring at
exactly the same place) and random errors in both Aeolus winds and radar winds, so we would expect them to be higher than
for the Aeolus winds themselves.

Acknowledgements

200 This work was supported by the Swedish National Space Agency (grant nos. 125/18 and 279/18). ESRAD operation and
maintenance is provided by Esrange Space Center of Swedish Space Corporation. The team members at Maitri station for
the Indian scientific expedition to Antarctica (ISEA) and the Antarctic logistics division at NCPOR (India) are
acknowledged for providing necessary support for the operation of MARA.



Author contributions

205 SK, EB and PV develop and maintain the software and data processing for ESRAD. SC and KS were responsible for operating the MARA radar and providing the data. SK, EB and PV developed the codes for the radar–Aeolus comparison and conducted the data analysis. SK, EB and PV prepared the paper with contributions from all co-authors.

Financial support

This research has been supported by the Swedish National Space Agency (grant nos. 125/18 and 279/18).

210 References

Belova, E., Kirkwood, S., Voelger, P., Chatterjee, S., Satheesan, K., Hagelin, S., Lindskog, M., and Körnich, H.: Validation of Aeolus winds using ground-based radars in Antarctica and in northern Sweden, *Atmos. Meas. Tech.*, 14, 5415–5428, <https://doi.org/10.5194/amt-14-5415-2021>, 2021.

215 ESA: ADM-Aeolus Science Report, ESA SP-1311, 121 pp., https://esamultimedia.esa.int/docs/EarthObservation/SP-1311ADM-Aeolus_Final.pdf (last access: 28 June 2021), 2008.

Iglewicz, B. and Hoaglin, D. C.: *How to Detect and Handle Outliers*, American Society for Quality Control, Statistics Division, vol.16, ASQ Quality Press, 1993.

220 Lux, O., Lemmerz, C., Weiler, F., Marksteiner, U., Witschas, B., Rahm, S., Geiß, A., and Reitebuch, O.: Intercomparison of wind observations from the European Space Agency's Aeolus satellite mission and the ALADIN Airborne Demonstrator, *Atmos. Meas. Tech.*, 13, 2075–2097, <https://doi.org/10.5194/amt-13-2075-2020>, 2020.

Lux, O., Witschas, B., Geiß, A., Lemmerz, C., Weiler, F., Marksteiner, U., Rahm, S., Schäfler, A., and Reitebuch, O.: Quality control and error assessment of the Aeolus L2B wind results from the Joint Aeolus Tropical Atlantic Campaign, *Atmos. Meas. Tech.*, 15, 6467–6488, <https://doi.org/10.5194/amt-15-6467-2022>, 2022

225 Martin, A., Weissmann, M., Reitebuch, O., Rennie, M., Geiß, A., and Cress, A.: Validation of Aeolus winds using radiosonde observations and numerical weather prediction model equivalents, *Atmos. Meas. Tech.*, 14, 2167–2183, <https://doi.org/10.5194/amt-14-2167-2021>, 2021.



Ratynski, M., Khaykin, S., Hauchecorne, A., Wing, R., Cammas, J.-P., Hello, Y., and Keckhut, P.: Validation of Aeolus wind profiles using ground-based lidar and radiosonde observations at La Réunion Island and the Observatoire de Haute Provence, EGU sphere [preprint], <https://doi.org/10.5194/egusphere-2022-822>, 2022.

230 Reitebuch, O.: The Spaceborne Wind Lidar Mission ADM-Aeolus, *Atmos. Phys.*, 815–827, https://doi.org/10.1007/978-3-642-30183-4_49, 2012.

Reitebuch, O., Lemmerz, C., Lux, O., Marksteiner, U., Rahm, S., Weiler, F., Witschas, B., Meringer, M., Schmidt, K., Huber, D., Nikolaus, I., Geiß, A., Vaughan, M., Dabas, A., Flament, T., Stieglitz, H., Isaksen, L., Rennie, M., Kloe, J., and Parrinello, T.: Initial Assessment of the Performance of the First Wind Lidar in Space on Aeolus, *EPJ Web Conf.*, 237, 01010, <https://doi.org/10.1051/epjconf/202023701010>, 2020.

Rennie, M. and Isaksen, L.: The NWP impact of Aeolus Level-2B winds at ECMWF, Technical Memorandum ECMWF no. 864, <https://doi.org/10.21957/alift7mhr>, 2020.

240 Rennie, M. P., Isaksen, L., Weiler, F., Kloe, J., Kanitz, T., and Reitebuch, O.: The impact of Aeolus wind retrievals in ECMWF global weather forecasts, *Q. J. R. Meteorol. Soc.*, <https://doi.org/10.1002/qj.4142>, 2021.

Stoffelen, A., Pailleux, J., Källén, E., Vaughan, M., Isaksen, L., Flamant, P., Wergen, W., Andersson, E., Schyberg, H., Culoma, A., Meynard, R., Endemann, M., and Ingmann, P.: The Atmospheric Dynamics Mission for Global Wind Field Measurements, *B. Am. Meteorol. Soc.*, 86, 73–88, 2005.

245 Weiler, F., Rennie, M., Kanitz, T., Isaksen, L., Checa, E., de Kloe, J., Okunde, N., and Reitebuch, O.: Correction of wind bias for the lidar on board Aeolus using telescope temperatures, *Atmos. Meas. Tech.*, 14, 7167–7185, <https://doi.org/10.5194/amt-14-7167-2021>, 2021.

Wu, S., Sun, K., Dai, G., Wang, X., Liu, X., Liu, B., Song, X., Reitebuch, O., Li, R., Yin, J., and Wang, X.: Inter-comparison of wind measurements in the atmospheric boundary layer and the lower troposphere with Aeolus and a ground-based coherent Doppler lidar network over China, *Atmos. Meas. Tech.*, 15, 131–148, <https://doi.org/10.5194/amt-15-131-2022>, 2022.

250